Energy Engineering

Tech Science Press

DOI: 10.32604/ee.2022.017273

ARTICLE

Establishment of a Coupling Model for the Prediction of Heat Dissipation of the Internal Combustion Engine Based on Finite Element

Hongyu Mu[1,2,*], Yinyan Wang[1], Hong Teng[2], Xingtian Zhao[2], Xiaolong Zhang[2], Yan Jin[2], Shiyang Hao[2] and Jingfeng Zhao[2]

[1]College of Power and Energy Engineering, Harbin Engineering University, Harbin, 150001, China

[2]Engine Department, R&D Center, Harbin Dongan Auto Engine Co., Ltd., Harbin, 150066, China

*Corresponding Author: Hongyu Mu. Email: muhongyu@hrbeu.edu.cn

Received: 27 April 2021 Accepted: 12 August 2021

ABSTRACT

The aerodynamics and heat transfer performance in the rear-mounted automobile cabin have an important influence on the engine's safety and the operational stability of the automobile. The article uses STAR-CCM and GT-COOL software to establish the 3D wind tunnel model and engine cooling system model of the internal combustion engine. At the same time, we established a 3D artificial coupling model through parameter transfer. The research results show that the heat transfer coefficient decreases with the increase of the comprehensive drag coefficient of the nacelle. This shows that the cabin flow field has an important influence on the heat transfer coefficient. The mainstream temperature rise of the engine room increases with the increase of the engine load. It is proved that vehicle speed affects the amount of heat dissipation of the engine room internal combustion engine under certain load conditions. The article provides a more effective and fast calculation method for the research on the heat dissipation of the internal combustion engine and the optimization of the cooling system equipment.

KEYWORDS

Internal combustion engine; coupled model; prediction; heat dissipation; heat dissipation of the whole machine

1 Introduction

The heat dissipation of the whole internal combustion engine and the heat dissipation of various internal combustion engines are affected by many complicated factors. Factors include combustion in the cylinder, the flow of air, coolant, lubricating oil, fuel, internal combustion engine structure, working conditions, external cooling system, environment, and so on. The academic circle has a set of mature theories and methods in internal combustion engine heat dissipation research. The primary method is to rely on the combination of experiment and simulation analysis to provide a design basis and optimization method for the engine compartment heat dissipation in the automotive development process. This paper conducts an experimental study on the performance of the internal combustion engine radiator, and the process will be explained

in detail later [1]. This paper conducts an experimental study on the performance of the internal combustion engine radiator, and the process will be explained in detail later. Due to the high cost of the experimental test and the extended period [2], it is impossible to analyze the heat flow field of the engine room comprehensively. We used CFD technology to simulate the flow field of the engine room [2], and this method successfully improved the heat dissipation performance of the engine room. It comprehensively considers convective heat transfer and radiation heat transfer in the engine room [3]. They did further research on the heat dissipation performance of the engine room. However, the calculation results are not ideal due to the consideration of radiation factors. Unreasonable radiation model settings may cause this. The flow field outside the car has an important influence on the air in the cabin. Considering the influence of the external flow field, when it established a CFD model of the entire vehicle external flow field, including the internal flow field of the engine room [4]. It accurately simulated the airflow conditions outside the engine room and inside the engine room.

Current internal combustion engine problems include calculation of internal combustion engine performance, including fluid flow and combustion, heat transfer and temperature field of components, lubrication and cooling systems, etc. Mature software is available now. We can directly use these local problem models and the coupling relationship between the boundary conditions of each model to establish a unified coupling model. This can significantly reduce the demand for thermal boundary conditions and improve the accuracy of calculation estimates. In addition, to further improve the availability of calculation results, we still need test data of similar reference prototypes. Based on the test data of the existing high-supercharged 4-cylinder internal combustion engine, this paper adjusts the coupling model to calculate the boundary conditions to estimate the heat dissipation of the internal combustion engine.

2 Multi-Model Coupling Method of Internal Combustion Engine

Fig. 1 shows the block diagram of the coupling relationship among the leading local models in the prediction and calculation of the heat dissipation of the internal combustion engine. It uses computer programs to realize data processing, connection, and adjustment between models.

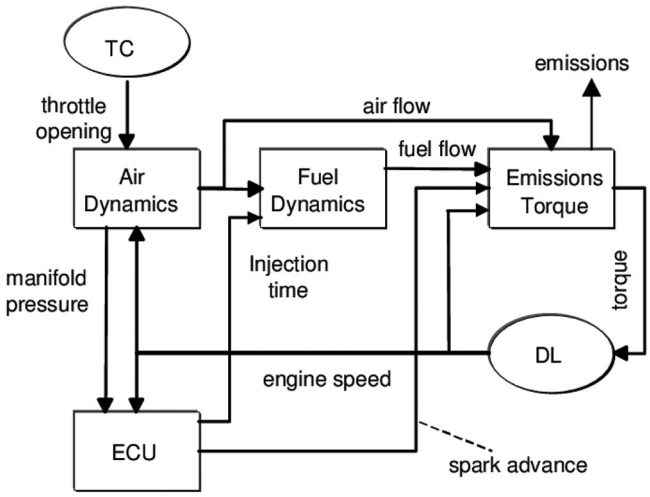

Figure 1: Block diagram of the coupling relationship between the main models of internal combustion engines

The heat flow of the whole machine and its distribution are calculated by loop iteration. Many boundary conditions of each local model are interrelated. For example, the time and space average temperature of the surface of the combustion chamber parts required for the performance calculation of the internal combustion engine can be obtained by the integral calculation of the spatial temperature distribution of the parts obtained by the finite element calculation of the temperature field of the parts. The transient temperature and heat transfer coefficient in the cylinder obtained by the performance calculation can be processed by time average and spatial distribution to obtain the boundary temperature and heat transfer conditions required for the finite element calculation of the part.

2.1 Empirical Parameter Method for Internal Combustion Engine Heat Dissipation

The empirical parameter method takes the rated power of the engine as the design working condition. The calculation of the target heat dissipation of the internal combustion engine is shown in Eq. (1). According to the engine's rated power, the windward area of the internal combustion engine is designed as shown in Eq. (2). The calculation of the total heat exchange area of the internal combustion engine is shown in Eq. (3).

$$Q = C_1 g_e P \frac{h_n}{3600} 1.1 \tag{1}$$

$$S_{wind} = (0.0027 \sim 0.0034) P \tag{2}$$

$$s_{total} = C_2 P \tag{3}$$

Q represents the target heat dissipation of the internal combustion engine, kW; C_1 represents the percentage of heat transferred to the cooling system in the fuel heat, and the value range is 0.18–0.25; g_e represents the gasoline consumption rate of the engine, and the value range is 0.210–0.270 kg/(KW·h); P represents the rated power of the engine, kW; h_n represents the low heating value of gasoline, hn = 41870 kJ/kg; S_{wind} represents the design windward area of the internal combustion engine core, m^2; C_2 represents the area of the heat dissipation ratio, according to passenger cars Experience, the value is 0.07 m^2/kW; S_{total} represents the total design heat dissipation area of the internal combustion engine, m^2.

The thesis assumes that Q_1 is the actual heat transfer amount of internal combustion engine heat dissipation; S_1 is the actual windward area, which is the product of core height and core width; the actual total heat transfer area (S_2/m^2) is calculated as shown in Eq. (4). When the wind is facing $Q_1 \geq Q, S_1 \geq S_{wind}, S_2 \geq S_{total}$, the cooling design of the internal combustion engine meets the design requirements.

$$S_2 = 2S_f + S_t \tag{4}$$

The formula S_f represents the heat dissipation area of the heat sink m^2; S_t represents the heat dissipation area of the flat tube m^2. The rated power is not commonly used during the everyday driving of a passenger car, and the speed at this operating point is relatively high. This design is conducive to heat dissipation. According to the rated power matching, the heat dissipation of the internal combustion engine is prone to the problem that the design heat dissipation capacity of the internal combustion engine heat dissipation is too large.

2.2 The Coupling Relationship between Internal Combustion Engine Performance and Piston, Cylinder Head, and Valve

2.2.1 Calculation Requirements for Internal Combustion Engine Performance

The average temperature $T_{wp}^{st}, T_{wh}^{st}, T_{wv}^{st}$, of the surface of the combustion chamber parts is uniformly expressed as T_w^{st}; the spatial average value $T_z^s(t), T_z^s(t)$ of the transient temperature and heat transfer coefficient in the output cylinder [5].

2.2.2 The Steady-State Temperature Field and Heat Flow Calculation Requirements of the Heated Parts of the Internal Combustion Engine

The time average temperature and time average heat transfer coefficient $T_z^t(s), T_z^t(s)$ of various parts of the combustion chamber. The average time temperature $T_{wp}^t(s), T_{wh}^t(s), T_{wv}^t(s)$ of the heated surface of the output combustion chamber parts is uniformly denoted as $T_w^t(s)$ [6]. For performance calculation requirements:

$$T_w^{st} = \int_s T_w^t(s)ds / \int_s ds \tag{5}$$

For the calculation requirements of the temperature field of the parts:

$$\begin{aligned} T_z^t(s) &= f_T^t(s) \cdot \textstyle\int_0^{t_c} T_z^s(t)dt/tc \\ T_z^t(s) &= f_T^t(s) \cdot \textstyle\int_0^{t_c} T_z^s(t) \end{aligned} \tag{6}$$

$$T_z^s(s) = dt / \int_0^{t_c} T_z^s(t)dt \tag{7}$$

Among them, T represents temperature, T represents surface heat transfer coefficient, and B represents pressure. W stands for oil film thickness t_c stands for duty cycle time, n stands for speed, t_{v1} stands for valve opening time, t_{v2} stands for valve closing time, A stands for the area, λ stands for thermal conductivity, h stands for height, s stands for space, and t stands for time [7].

The meanings of the superscripts appearing here in the text are as follows: s stands for spatial average; t stands for time average; subscripts: z stands for in-cylinder; w stands for part wall; p stands for piston; h stands for cylinder head; v stands for valve; c stands for cylinder liner; r stands for piston ring; g stands for valve sealing surface; o stands for lubricating oil [8].

2.3 Coupling Relationship among Internal Combustion Engine Performance, Valve and Cylinder Head

Let's take the exhaust valve as an example for analysis. The thermal coupling relationship between the valve and the cylinder head is mainly on the valve seat surface [9]. If the heat transfer coefficient function $T_g^s(t)$ of the seat surface during valve seat closing is known, then the time average temperature and heat transfer coefficient $T_{vg}^t(t), T_{vg}^t(s), T_{hg}^t(t), T_{hg}^t(s)$ on the valve sealing surface can be obtained coupling relationship. For the valve sealing surface [10]:

$$T_{vg}^t(s) = [(t_c - tv2 + tv1)T_{hg}^t(s) + \int_{t_{v1}}^{t_{v2}} T_z^s(t)dt]/t_c \tag{8}$$

$$T_{vg}^t(s) = [\int_{t_c-(t_{v1},t_{v2})} T_g^s(t)T_{hg}^t(s)dt + \int_{t_{v1}}^{t_{v2}} T_z^s(t)dt]/(t_c T_{vg}^t(s)) \tag{9}$$

For the sealing surface of the cylinder head valve seat ring:

$$T_{hg}^{t}(s) = [(t_c - t_{v2} + t_{v1})T_{vg}^{t}(s) + \int_{t_{v1}}^{t_{v2}} T_z^s(t)dt]/t_c \tag{10}$$

$$T_{hg}^{t}(s) = [\int_{t_c-(t_{v1},t_{v2})} T_g^s(t)T_{vg}^{t}(s)dt + \int_{t_{v1}}^{t_{v2}} T_z^s(t)dt]/(t_c T_{hg}^{t}(s)) \tag{11}$$

2.4 *The Coupling Relationship among Internal Combustion Engine Performance, Piston, Piston Ring, Piston Ring Lubricant Film, and Cylinder Liner*

The temperature $T_{wc}^{t}(s)$ of the inner surface of the cylinder liner can be calculated by the temperature field, and the area $A_{wc}(t)$ of the contact part between the cylinder liner and the gas in the cylinder at any time t can be obtained by the piston kinematics relationship. The average heat transfer area A_{wc}^{ts} and the average wall temperature T_{wc}^{ts} can be obtained by the following formula [11]:

$$A_{wc}^{ts} = \int_0^{t_c} A_{wc}(t) \cdot dt/t_c \tag{12}$$

$$T_{wc}^{ts} = \int_0^{t_c} \int_s T_{wc}^{t}(s) \cdot A_{wc}(t,s) \cdot dsdt/A_{wc}^{ts} \cdot t_c \tag{13}$$

We use the finite difference method to solve the Reynolds lubrication equation to calculate the thickness of the lubricating oil film between the piston ring and the cylinder liner. Fig. 2 is a schematic diagram of the heat transfer and heat conduction relationship between the piston ring groove-ring-oil film-cylinder liner of an internal combustion engine.

$$L_r = W_0 + l_r + W_2 \tag{14}$$

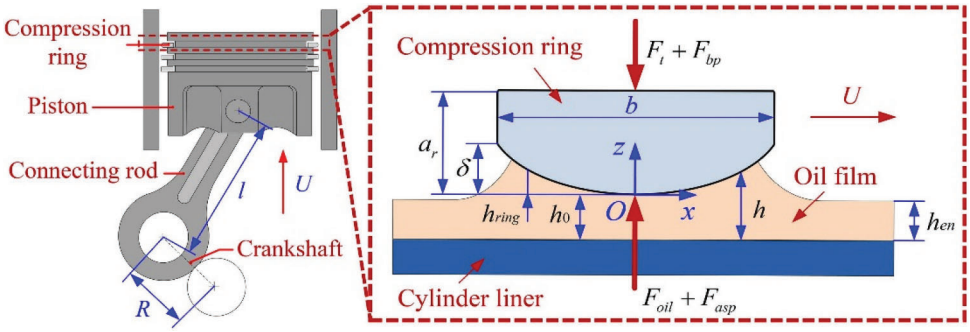

Figure 2: Coupling relationship of heat transfer and heat conduction of internal combustion engine piston ring groove-ring-oil film-cylinder liner

The coupling relationship between the bottom of the ring groove and the piston ring can adopt the first type boundary condition of complete contact. The heat transfer coefficient T_0 of the coupled boundary surface of the low pressurization or non-first ring can be expressed as

$$T_0 = 1/(W_p/\lambda_p + W_0/\lambda_0 + W_r/\lambda_r) \tag{15}$$

$W_p, \lambda_p + W_0, \lambda_0 + W_r, \lambda_r$ are the average height of the piston, oil film, and piston ring, and the material's thermal conductivity, respectively. The heat transfer environment at a particular point x on the cylinder liner will change with time. It may contact gas, piston firepower bank, piston first ring, piston ring bank, piston second ring,…, piston skirt, oil mist in the crankcase. We assume that this point has experienced different heat transfer environments in the i section. In this way, we can calculate the time t_i and the average ambient temperature T_i for these sections to sweep through point x in each cycle. We can use the temperature on the piston as the average ambient temperature when certain sections of the piston sweep past point x. Then the average ambient temperature and equivalent heat transfer coefficient at point x in a working cycle of the internal combustion engine are T_e and T_e.

$$T_e = \sum T_i \cdot t_i \Big/ \sum t_i \tag{16}$$

$$T_e = \sum T_i \cdot (T_i - T_x) \cdot t_i \Big/ \left[(T_e - T_x) \cdot \sum t_i \right] \tag{17}$$

2.5 *Mathematical Model of Internal Combustion Engine Heat Transfer Coefficient*

The mathematical model of internal combustion engine heat dissipation is based on the ε-NTU method. The actual heat exchange amount can be expressed by Eq. (18) [12]. The key to the heat transfer calculation is the heat transfer efficiency ε. ε is a function of the Nusselt number Nu. According to the test data of the internal combustion engine heat dissipation bench, the paper uses Reynolds number (Re) and Prandtl number (Pr) to fit Nu. The specific data is shown in Eq. (19).

$$P_{\text{Heatexchange}} = \text{C}_{\min} |\text{T}_{in1} - T_{in2}| \varepsilon \tag{18}$$

$$Nu = \alpha \text{Re}^{\beta} \text{Pr}^{\gamma} \tag{19}$$

In the formula: $P_{\text{Heatexchange}}$ represents the heat exchange amount, kW; $\text{C}_{\min}$ represents the smaller specific heat capacity flow rate of the two heat exchange fluids, kW/°C; T_{in1} represents the air inlet temperature, °C; T_{in2} represents the coolant inlet temperature, °C; ε represents Heat transfer efficiency, %; Nu means Nusselt number; Re means Reynolds number; Pr means Prandtl number; α, β and γ indicate fitting coefficients [13].

3 Thermal Model Design

3.1 *Model-Based Optimization Design Scheme*

In the original scheme, the low-speed climbing engine has a low equilibrium water temperature, and the internal combustion engine has a large heat dissipation margin. Initially, the optimized size of the internal combustion engine heat dissipation core was set at 703 mm × 440 mm × 16 mm. We reduced the core thickness of internal combustion engine heat dissipation by 11 mm. The size comparison of the two schemes is shown in Table 1 [14]. We substitute the performance data and geometric dimensions of the optimized solution into the model for calculation.

Table 1: Thermal parameters of the internal combustion engine (mm)

Geometric parameters	Original plan	Optimization
Flat tube height	1.5	1.5
Flat tube material thickness	0.22	0.22
Fin wave height	5	5
Fin pitch	2.4	2.4
Fin material thickness	0.07	0.07
Fin efficiency	0.85	0.85

3.2 Fitting of the Heat Transfer Coefficient of the Internal Combustion Engine Optimization Scheme

Table 2 shows the single product performance data of the internal combustion engine optimization program. The performance is tested according to national standards on the heat transfer performance test bench under the condition of a temperature difference between liquid and gas inlet of 60°C. The Nusselt number calculation formula is fitted by the performance data of the single product of the internal combustion engine heat dissipation bench test, as shown in Eqs. (20)–(23) [15]. Then calculate the simulated heat dissipation. This can be used to calculate the heat transfer in actual road conditions [16].

$$Nu_{1la\min ar} = 0.0761\mathrm{Re}^{0.8852^{0.2903}}\mathrm{Pr} \tag{20}$$

$$Nu_{1lturbulent} = 1.01\mathrm{Re}^{0.502^{0.3333}}\mathrm{Pr} \tag{21}$$

$$Nu_{2la\min ar} = 0.667\mathrm{Re}^{0.4211^{0.0503}}\mathrm{Pr} \tag{22}$$

$$Nu_{2lturbulent} = 1.012\mathrm{Re}^{0.501^{0.3333}}\mathrm{Pr} \tag{23}$$

Table 2: Single product performance parameter table of a particular model of internal combustion engine heat dissipation optimization plan

Working condition point number	Wind speed (m/s)	Water flow rate (L/min)	Heat dissipation (kW)
1	2	40	24.3
2	2	60	26.8
3	2	80	27.2
4	2	100	28.1
5	4	40	36.3

(Continued)

Table 2 (Continued)

Working condition point number	Wind speed (m/s)	Water flow rate (L/min)	Heat dissipation (kW)
6	4	60	41.2
7	4	80	43.8
8	4	100	45.5
9	6	40	41.8
10	6	60	49.6
11	6	80	53.9
12	6	100	56.8
13	8	40	45.2
14	8	60	55.2
15	8	80	61.2
16	8	100	65.4

In the formula: $Nu_{1la\min ar}$ represents the laminar flow Nusselt number on the wind side; $Nu_{1lturbulent}$ represents the turbulent Nusselt number on the wind side; $Nu_{2la\min ar}$ represents the laminar flow Nusselt number on the waterside; $Nu_{2la\min ar}$ represents the turbulent Nusselt number on the waterside [17].

4 Experimental Research

4.1 Limit Steady-State Simulation and Test Results Analysis

The parameters of low-speed climbing conditions and high-speed climbing conditions are shown in Table 3. The wind speed and wind temperature distribution of the internal combustion engine before the heat is dissipated are input by the 3D CFD simulation analysis results [18].

Table 3: Test condition parameter table of limit steady-state conditions

Parameter name	Low-speed climbing	High-speed climbing
Environment temperature (°C)	40	45
Vehicle speed (km/h)	40	120
Road slope (%)	10	3
Engine speed (r/min)	1629	2564
Transmission gear	3	7

The simulation result of the equilibrium water temperature of the engine water outlet is shown in Fig. 3. The balanced water temperature at the outlet of the engine for low-speed climbing is 113.4°C, and for high-speed climbing, it is 114.8°C, which meets the design water temperature limit (115°C).

We load the new sample into a car for a ring mold test [19]. The results of the actual car test are shown in Fig. 4. In the optimized scheme, the equilibrium water temperature of the engine outlet for low-speed climbing is 113.1°C, and that for high-speed climbing is 115.0°C, which meets the design water temperature limit (115°C). The balance water temperature error of low-speed

climbing is 0.26%, and the error of high-speed climbing conditions is 0.17%, indicating that the simulation results are more accurate.

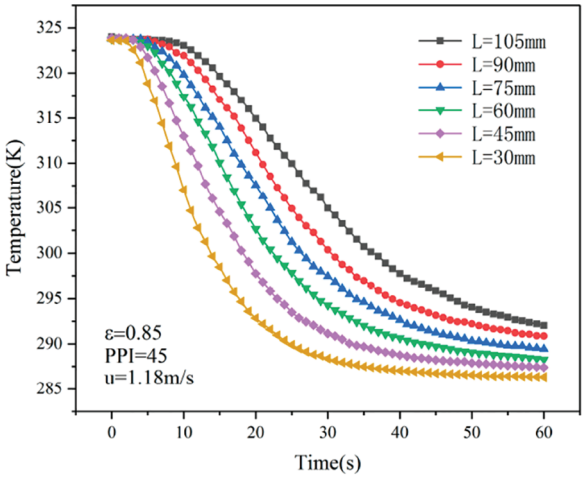

Figure 3: Simulation curve of the equilibrium temperature of engine water outlet under steady-state conditions

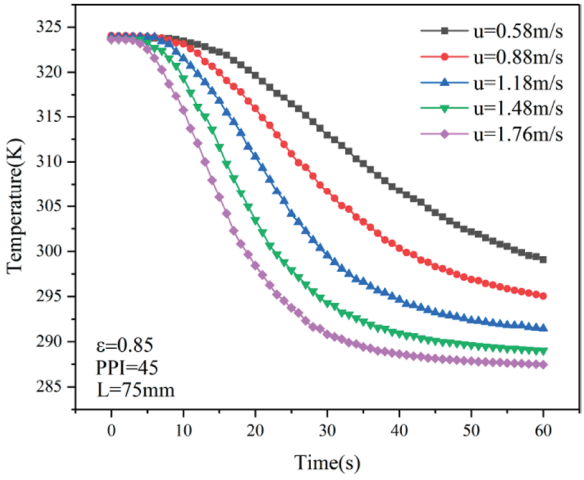

Figure 4: Test curve of the equilibrium temperature of engine water outlet under steady-state conditions

The balance water temperature of the low-speed climbing of the new internal combustion engine heat dissipation scheme designed in the thesis has increased by 16.3°C, while meeting the design limit of 115°C. The heat dissipation quality of the internal combustion engine is reduced by 1.2 kg. This achieves the goal of reducing the heat dissipation of the internal combustion engine and the optimal cooling system performance.

4.2 Prediction Basis and Simulation of Prediction Results

The article calculates the performance and boundary conditions of the newly designed diesel engine to extrapolate and predict the heat dissipation of the whole engine and the distribution of heat dissipation of various parts. The heat dissipation of the whole machine is calculated from formulas (1) to (12). Table 4 shows the calculation results of heat dissipation adjustment of the existing 4-cylinder supercharged 290 kW diesel engine. Table 5 shows the prediction results of the heat dissipation of the newly designed 4-cylinder supercharged 360 kW diesel engine. Fig. 5 shows the results of finite element analysis to predict heat dissipation of the internal combustion engine.

Table 4: Calculation results of heat dissipation adjustment of the existing 4-cylinder supercharged 290 kW diesel engine

Project name	Heat dissipation value (kW)	Project name	Heat dissipation value (kW)
Total heat transfer of piston	29.7	Total heat dissipation of exhaust valve	2.9
The amount of heat dissipated from the piston to the oil	23.7	Heat dissipation from the valve seat to the cylinder head	2.5
Total heat dissipation of cylinder liner	53.9	Total heat dissipation through cooling water	108.8
Heat dissipation from the piston to the cylinder liner	6.0	Total heat dissipation through oil	38.1
Total heat dissipation of cylinder head	57.9	Total heat dissipation through the air	62.9
Cylinder head exhaust duct heat dissipation	37.1	Total heat dissipation of engine	209.8

Table 5: Forecast results of heat dissipation of the newly designed 4-cylinder supercharged 360 kW diesel engine

Project name	Heat dissipation value (kW)	Project name	Heat dissipation value (kW)
Total heat transfer of piston	35.2	Total heat dissipation of exhaust valve	3.5
The amount of heat dissipated from the piston to the oil	28.3	Heat dissipation from the valve seat to the cylinder head	3.0
Total heat dissipation of cylinder liner	60.2	Total heat dissipation through cooling water	125.6

(Continued)

Table 5 (Continued)

Project name	Heat dissipation value (kW)	Project name	Heat dissipation value (kW)
Heat dissipation from the piston to the cylinder liner	6.9	Total heat dissipation through oil	44.9
Total heat dissipation of cylinder head	68.7	Total heat dissipation through the air	82.2
Cylinder head exhaust duct heat dissipation	44.0	Total heat dissipation of engine	252.7

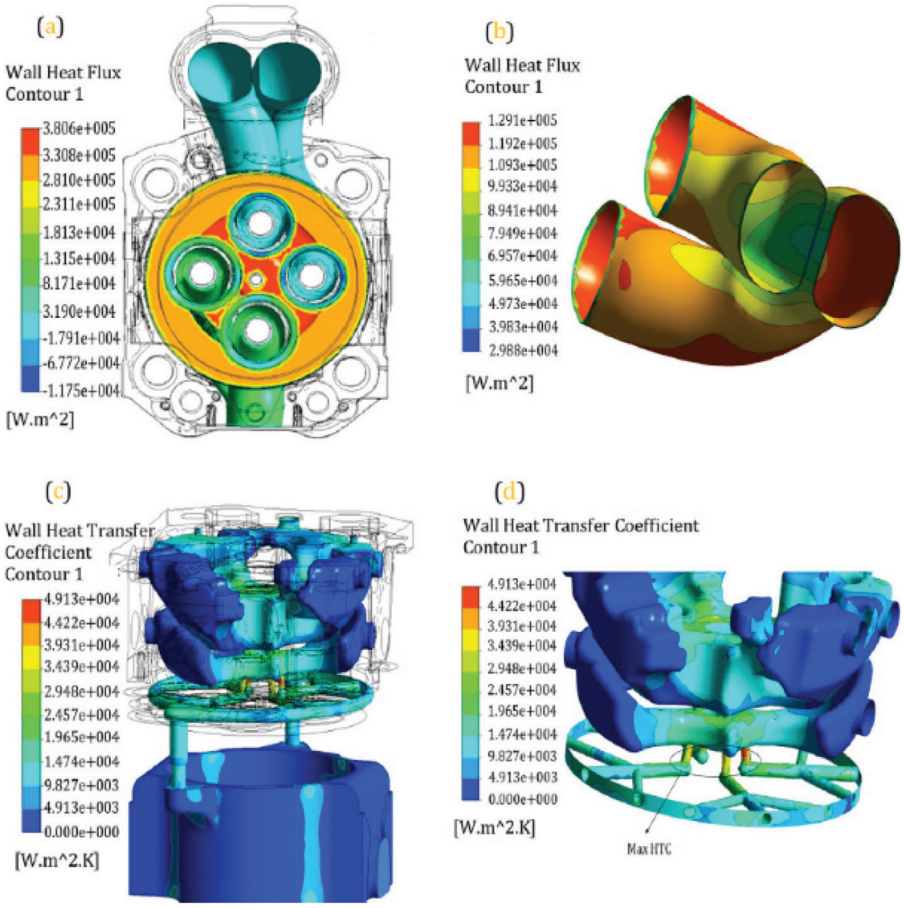

Figure 5: Finite element analysis results for the prediction of heat dissipation of the entire internal combustion engine

It can be seen from Table 6 that after adopting the scheme in this paper, compared with the algorithm proposed in [20]. The heat dissipation efficiency of the radiator has increased. About 20%, the heat dissipation efficiency of the entire cooling system and engine has also increased by

about 15%. In the entire cooling system in the engine compartment, the intercooler and radiator are used most frequently.

Table 6: Comparative analysis of the scheme in this paper and literature [20] (W/s)

	This article scheme	Literature [20]	Heat dissipation efficiency change(%)
Intercooler heat dissipation	50568.4219	48220.8906	−4.64
Heat dissipation capacity of the radiator	167450.9032	214101.5938	21.79
Condenser heat dissipation	17562.9809	13528.5928	−29.82
Engine heat dissipation	7209.0746	7833.1178	7.97
Total heat dissipation	242790.7836	283684.195	14.42
Maximum temperature of temperature field (°C)	74.98	83.78	11.74

5 Conclusion

In the process of predicting the heat dissipation of the whole machine, the coupling boundary conditions between the models and parts can be determined more accurately through the coupling relationship between the models and calculation iterations. This shows that the analysis model and analysis method are correct. The cooling constant of the radiator at the rated power point is lower than the design index. This shows that the selection of the parameters of the fan and the radiator matching the engine is not feasible. The maximum temperature of the engine compartment temperature field at the rated power point and the maximum torque point did not reach the maximum allowable operating temperature of the engine compartment 90°C. The maximum temperature of the air in the engine compartment is controlled within the design index value. This shows that the temperature field characteristics in the engine compartment meet the design requirements.

Funding Statement: The study was partly supported by the Grant SC2021ZX05A0013 of the Heilongjiang Province "hundred, thousand, thousand" Engineering Science and Technology Major Special Project.

Conflicts of Interest: The authors declare that they have no conflicts of interest to report regarding the present study.

References

1. Polat, S., Solmaz, H., Calam, A., Yilmaz, E. (2020). Estimation of the COVIMEP variation in a HCCI engine. *Politeknik Dergisi, 23(3),* 721–727. DOI 10.2339/politeknik.567865.
2. ElBahloul, M. A., Aziz, E. S., Chassapis, C. (2019). Mechanical efficiency prediction methodology of the hypocycloid gear mechanism for internal combustion engine application. *International Journal on Interactive Design and Manufacturing, 13(1),* 221–233. DOI 10.1007/s12008-018-0508-2.
3. ElBahloul, M. A., Aziz, E. S., Chassapis, C. (2021). Performance study of the hypocycloid gear mechanism for internal combustion engine applications. *International Journal of Engine Research, 22(4),* 1222–1238. DOI 10.1177/1468087419893583.

4. Luján, J. M., Dolz, V., Monsalve-Serrano, J., Bernal Maldonado, M. A. (2021). High-pressure exhaust gas recirculation line condensation model of an internal combustion diesel engine operating at cold conditions. *International Journal of Engine Research, 22(2),* 407–416. DOI 10.1177/1468087419868026.
5. Zhu, H., Zhang, Y., Liu, F., Wei, W. (2020). Effect of excess hydrogen on hydrogen fueled internal combustion engine under full load. *International Journal of Hydrogen Energy, 45(39),* 20419–20425. DOI 10.1016/j.ijhydene.2019.12.022.
6. Pla, B., de la Morena, J., Bares, P., Jiménez, I. (2020). Cycle-to-cycle combustion variability modelling in spark ignited engines for control purposes. *International Journal of Engine Research, 21(8),* 1398–1411. DOI 10.1177/1468087419885754.
7. Wang, X., Sun, B. G., Luo, Q. H. (2019). Energy and exergy analysis of a turbocharged hydrogen internal combustion engine. *International Journal of Hydrogen Energy, 44(11),* 5551–5563. DOI 10.1016/j.ijhydene.2018.10.047.
8. Malé, Q., Staffelbach, G., Vermorel, O., Misdariis, A., Ravet, F. et al. (2019). Large eddy simulation of pre-chamber ignition in an internal combustion engine. *Flow, Turbulence and Combustion, 103(2),* 465–483. DOI 10.1007/s10494-019-00026-y.
9. Li, Y., Gao, W., Zhang, P., Ye, Y., Wei, Z. (2019). Effects study of injection strategies on hydrogen-air formation and performance of hydrogen direct injection internal combustion engine. *International Journal of Hydrogen Energy, 44(47),* 26000–26011. DOI 10.1016/j.ijhydene.2019.08.055.
10. Gainey, B., Longtin, J. P., Lawler, B. (2019). A guide to uncertainty quantification for experimental engine research and heat release analysis. *SAE International Journal of Engines, 12(5),* 509–290. DOI 10.4271/03-12-05-0033.
11. Thawko, A., Yadav, H., Eyal, A., Shapiro, M., Tartakovsky, L. (2019). Particle emissions of direct injection internal combustion engine fed with a hydrogen-rich reformate. *International Journal of Hydrogen Energy, 44(52),* 28342–28356. DOI 10.1016/j.ijhydene.2019.09.062.
12. Zhu, H., Duan, J. (2019). Research on emission characteristics of hydrogen fuel internal combustion engine based on more detailed mechanism. *International Journal of Hydrogen Energy, 44(11),* 5592–5598. DOI 10.1016/j.ijhydene.2018.08.044.
13. Franken, T., Klauer, C., Kienberg, M., Matrisciano, A., Mauss, F. (2020). Prediction of thermal stratification in an engine-like geometry using a zero-dimensional stochastic reactor model. *International Journal of Engine Research, 21(9),* 1750–1763. DOI 10.1177/1468087418824217.
14. Liu, X., Reddi, K., Elgowainy, A., Lohse-Busch, H., Wang, M. et al. (2020). Comparison of well-to-wheels energy use and emissions of a hydrogen fuel cell electric vehicle relative to a conventional gasoline-powered internal combustion engine vehicle. *International Journal of Hydrogen Energy, 45(1),* 972–983. DOI 10.1016/j.ijhydene.2019.10.192.
15. Rajak, U., Verma, T. N. (2020). Influence of combustion and emission characteristics on a compression ignition engine from a different generation of biodiesel. *Engineering Science and Technology, an International Journal, 23(1),* 10–20. DOI 10.1016/j.jestch.2019.04.003.
16. Han, D., Zhai, J., Huang, Z. (2019). Autoignition of *n*-hexane, cyclohexane, and methylcyclohexane in a constant volume combustion chamber. *Energy & Fuels, 33(4),* 3576–3583. DOI 10.1021/acs.energyfuels.9b00003.
17. Nigay, N. A., Kuznetsov, G. V., Syrodoy, S. V., Gutareva, N. Y. (2020). Estimation of energy consumption for drying of forest combustible materials during their preparation for incineration in the furnaces of steam and hot water boilers. *Energy Sources, Part A: Recovery, Utilization, and Environmental Effects, 42(16),* 1997–2005. DOI 10.1080/15567036.2019.1604910.
18. Arat, H. T. (2019). Alternative fuelled hybrid electric vehicle (AF-HEV) with hydrogen enriched internal combustion engine. *International Journal of Hydrogen Energy, 44(34),* 19005–19016. DOI 10.1016/j.ijhydene.2018.12.219.

19. Namar, M. M., Jahanian, O. (2019). Energy and exergy analysis of a hydrogen-fueled HCCI engine. *Journal of Thermal Analysis and Calorimetry, 137(1),* 205–215. DOI 10.1007/s10973-018-7910-7.
20. Piscaglia, F., Onorati, A., Marelli, S., Capobianco, M. (2019). A detailed one-dimensional model to predict the unsteady behavior of turbocharger turbines for internal combustion engine applications. *International Journal of Engine Research, 20(3),* 327–349. DOI 10.1177/1468087417752525.